

Attenuation of obesity-induced inflammation in mice orally administered with salmon
cartilage proteoglycan, a prophylactic agent

(サケ鼻軟骨抽出プロテオグリカンの経口投与は肥満由来の炎症を軽減する)

申請者 弘前大学大学院医学研究科
病態制御科学領域感染生体防御学教育研究分野

氏名 廣瀬 昌平
指導教授 若林 孝一

Abstract

Obesity is associated with chronic inflammation of adipose tissue and causes development of type 2 diabetes. M1 macrophage population was increased in adipose tissue of obese mouse. M1 macrophages induce insulin resistance through the secretion of proinflammatory cytokines. Our previous studies demonstrated that salmon cartilage proteoglycan (PG) suppresses excess inflammation in various mouse inflammatory diseases. In this study, we examined the effect of PG on type 2 diabetes using high-fat-diet (HFD) induced obese mouse model. Oral PG administration enhanced the population of small adipocytes (area less than 1000 μm^2) without body and tissue weight gain. In addition, PG administration suppressed mRNA expression of TNF- α , IL-6 and CXCL2 in adipose tissue. The proportion of M1 macrophages was decreased by PG administration. In addition, PG administration suppressed hyperglycemia after intraperitoneal glucose injection. Fasted serum insulin level was decreased in PG-administered mice. Moreover, insulin-stimulated phosphorylation of Akt was enhanced in the liver and gastrocnemius skeletal muscle of PG-administered mice. These data suggested that PG administration improves hyperglycemia and insulin sensitivity in obese mice by modulation of M1 macrophages which secrete proinflammatory cytokines in adipose tissue and activation of

Akt in liver and skeletal muscle.

Introduction

In modern society, high consumption of energy-dense foods has led to a substantial increase in overweight and obese persons. It is increasingly accepted that obesity is characterized by chronic inflammation of adipose tissues, which causes development of insulin resistance and type-2 diabetes [1]. In adipose tissues of obese persons, adipose tissue macrophages (ATMs) play important roles in inflammation [2-5]. While the population of ATMs in lean mice is around 5%, it increases up to 50% in obese mice [4]. Besides increasing number, localization and phenotype of ATMs are changed during development of obesity. Macrophages can be classified into two phenotypes as classically activated (M1) and alternatively activated (M2) macrophages. M1 macrophages activate microbicidal activity, whereas M2 macrophages participate in allergic and antiparasitic responses [6]. M1 macrophages infiltrate into obese adipose tissues and secrete excessive pro-inflammatory cytokines, such as tumor necrosis factor- α (TNF- α), which then induce the additional accumulation of macrophages in adipose tissues [7]. Moreover, in the context of insulin action, M1 macrophages induce insulin resistance through the secretion of pro-

inflammatory cytokines [8]. Therefore, to improve insulin resistance due to obesity-related inflammation, it is important to regulate the proportion of M1 macrophages and to reduce the production of pro-inflammatory cytokines in obese adipose tissue.

Proteoglycan (PG) consists of core protein with one or more covalently attached glycosaminoglycan chain(s). It is a compound of extracellular matrix materials that exists in connecting tissue such as skin, bone, cartilage and vascular wall by forming a complex with collagen, fibronectin, laminin, hyaluronic acid and other glycoproteins. In corporation with collagen, fibronectin and laminin, PG has been shown to be involved in cellular proliferation and adhesion [9]. We have previously demonstrated that PG extracted from salmon nasal cartilage has a potent effect on suppression of inflammatory responses induced by heat-killed *Escherichia coli* in mouse macrophages [10]. In addition, daily oral administration of PG attenuates the severity of experimental inflammatory colitis [11], autoimmune encephalomyelitis [12] and collagen-induced arthritis [13]. Our previous study also suggested that ingested PG may contribute to homeostasis of host immunity mediated through the balance in composition of gut microbiota [14].

Here, we report that PG has a prophylactic effect on obesity-related inflammation and blood

glucose level in C57BL/6J mice fed a high-fat diet (HFD). We demonstrated that PG reduced the production of pro-inflammatory cytokines and the proportion of M1 macrophages in obese adipose tissue. In addition, PG was able to improve hyperglycemia in diet-induced obese mice. These results suggest that PG may have a beneficial effect on obesity-induced inflammation.

Materials and methods

Animals and diets

Male C57BL/6 mice, 4 weeks old, were purchased from Clea Japan, Tokyo, Japan, and maintained in a temperature-controlled room (22°C) on a 12-h light-dark cycle at Institute for Animal Experimentation, Hirosaki University Graduate School of Medicine. Mice were either fed HFD (60% energy from fat) or received continuous feeding of a normal diet (ND) (5.6% energy from fat). Both diets were purchased from Clea Japan. All animal experiments were carried out in accordance with the Guidelines for Animal Experimentation of Hirosaki University. All mouse experiments were approved by the Committee on the Ethics of Animal Experimentation of Hirosaki University (permission number M10003).

PG administration

PG extracted from salmon nasal cartilage was purchased from Kakuhiro Co. Ltd, Aomori, Japan. Mice from HFD-fed group and ND-fed group were administered with 0.2 mg/ml PG through drinking distilled water (DW) for up to 16 weeks. DW only was used as a negative control. Body weight and food intake of mice were measured once two weeks and once a week, respectively. Adipose tissue and liver were isolated and their weights were measured from 16 week-fed mice.

Measurement of adipocyte area

After 16 weeks of feeding, epididymal adipose tissue was collected and fixed in 4% (w/v) paraformaldehyde buffer at 4°C for overnight. Tissues were then embedded in paraffin and cut into 5- μ m thick sections. Deparaffinized sections were stained with hematoxylin and eosin. The tissues were observed under BZ-X700 microscope (Keyence, Tokyo, Japan) and adipocyte area were measured from randomly selected cells (n=400).

Real-time quantitative reverse transcription-PCR (qRT-PCR).

Total RNAs from adipose tissues were isolated using TRIzol reagent (Invitrogen, Carlsbad, CA) according to the manufacturer's instruction. First-strand cDNAs were synthesized from 1 μ g total RNA using random primers (Takara, Shiga, Japan) and Moloney murine leukemia virus reverse transcriptase (Invitrogen). The primers used to amplify target genes from cDNA are listed in Table 1. PCRs were run at the following conditions: initial activation of Taq DNA polymerase at 95°C for 5 min, 40 cycles of 30 sec at 95°C for denaturing, 30 sec at 60°C for annealing, and 30 sec at 72°C for elongation. Gene expression levels were determined by real-time qPCR analysis using the SYBR green Supermix (Bio-Rad Laboratories, San Jose, CA). Dissociation curves were used to detect primer-dimer conformation and nonspecific amplification. The detection threshold was set to the log linear range of the amplification curve and kept constant (0.05) for all data analysis. The threshold cycle (C_T) of each target product was determined and set in relation to the amplification plot of glyceraldehyde 3-phosphate dehydrogenase (GAPDH). The difference between the C_T values (ΔC_T) of two genes was used to calculate the relative expression; i.e., relative expression = $2^{-(C_T \text{ of target gene} - C_T \text{ of GAPDH})} = 2^{-\Delta C_T}$.

Preparation of adipose-derived cells in the stromal vascular fraction

Adipose tissue was placed into RPMI1640 medium (Nissui Pharmaceutical Co., Tokyo, Japan) and digested with 0.3 units/ml collagenase IA (Roche Applied Science, Indianapolis, IN) at 37°C for 40 min. The cells obtained were passed through a sterile 100 µm strainer (Fischer Scientific, Franklin, MA), and collected by centrifugation (500×g) at 4°C for 10 min. After hemolysis, cells in the stromal vascular fraction (SVF) were resuspended and kept in staining buffer [phosphate-buffered saline (PBS) containing 1 mM EDTA, 25 mM HEPES, and 1% (w/v) fatty acid-free bovine serum albumin (BSA, fraction V, Sigma-Aldrich Japan Inc., Tokyo, Japan)] until immunolabeling.

Flow cytometry

Macrophages in the SVF were stained with fluorescein isothiocyanate (FITC)-conjugated rat anti-mouse F4/80 monoclonal antibody (mAb, eBioscience, San Diego, CA), phycoerythrin (PE)-conjugated rat anti-mouse CD11c mAb (Biolegend, San Diego, CA), and Alexa647-conjugated rat anti-mouse CD206 mAb (Biolegend) or isotype controls (BD Biosciences, San Jose, CA). Fluorescent intensity was analyzed by FACSCanto™ II flow cytometer (BD Biosciences).

Immunohistochemical analysis

After 8 weeks of feeding, epididymal adipose tissue was collected and fixed in 4% (w/v) paraformaldehyde buffer at 4°C for overnight. Tissues were soaked in PBS containing 30% sucrose and they were frozen in optimal cutting temperature medium (Sakura Finetek Japan, Tokyo, Japan) at -80°C. Frozen tissues were sliced into 10 µm, washed with PBS and incubated with 2% (v/v) normal rat serum in PBST [0.05% (v/v) Tween 20 in PBS] for 30 min at room temperature. Then, the sections were rinsed with PBST and double stained with FITC-conjugated anti-mouse F4/80 mAb (0.2 µg/ml) and PE-conjugated anti-mouse CD11c mAb (0.2 µg/ml) or Alexa647-conjugated anti-mouse CD206 mAb (0.2 µg/ml) at 4°C for 16 h. After rinse with PBST, the sections were counterstained with 4',6-diamidino-2-phenylindole (DAPI; Wako Pure Chemical Industries, Osaka, Japan) and coverslipped with Fluoromount (Life Technologies, Carlsbad, CA), and then they were observed under BZ-X700 microscope. Crown-like structures (CLSs) were randomly counted from seven histological sections.

Serum insulin measurement and intraperitoneal glucose tolerance test

Blood samples were obtained from 6 h-fasted mice at 12 week-feeding. Serum insulin level

was determined using mouse insulin ELISA kit (Morinaga Inst. Biol. Sci. Inc, Yokohama, Japan).

For intraperitoneal glucose tolerance test (IPGTT), 14 week-fed mice were fasted for 6 h and injected intraperitoneally with 20% glucose in PBS at a dose of 2 mg/g body weight. Then, blood samples were collected at 0, 15, 30, 60 and 120 min for glucose measurement using a Nipro stat strip XP (Nipro, Osaka, Japan).

Western blotting

8 week-fed mice were fasted for 6 h and injected intraperitoneally with insulin (2.0 U/kg body weight). Liver and gastrocnemius skeletal muscle were collected 10 min later and homogenized. The proteins were separated by SDS-PAGE and transferred to PVDF membrane. After blocking with 5% skim milk (Morinaga Milk Co., Tokyo, Japan) in PBST, Akt and phosphorylated Akt were detected using anti-Akt and anti-phospho-Akt (Ser473) antibodies (Cell Signaling Technology Inc., Beverly, MA), respectively. After incubation with horseradish peroxidase (HRP)-conjugated protein A (Bio-Rad Laboratories), chemiluminescence signals were visualized using ECL western blotting detection reagents (GE Healthcare Biosciences, Piscataway, NJ). Immunoblotted band intensity was quantified using Image Lab software (Bio-Rad Laboratories).

Statistical analysis

Data were expressed as means \pm standard deviations, and $P < 0.05$ from student's t test analysis was used to determine the significance of the differences.

Results

PG showed no significant effect on body weight, food intake or tissue weight.

To determine whether PG affects body weight and food intake, we measured these parameters during HFD or ND feeding with or without PG administration. Although body weight of HFD-fed mice was significantly higher than that of ND-fed mice, there was no significant difference in body weight or food intake between the PG-administered and the control mice (Fig. S1A). Tissues were then collected and weighed at 16 weeks after feeding. As expected, weights of the adipose tissue and liver of HFD-fed mice were significantly higher than those of ND-fed mice. In addition, there was no significant difference in tissue weights between the PG-administered group and the control group (Fig. S1B). However, the number of small adipose cells with the area less than 1000

μm^2 was increased in the PG administered HFD-fed mice when compared with the control HFD-fed mice (Fig. S1C).

PG suppressed mRNA expression of TNF- α , IL-6 and CXCL2 in adipose tissue.

To determine the anti-inflammatory effect of PG in adipose tissue, mRNA expression of proinflammatory cytokines was evaluated by qRT-PCR. We firstly assessed mRNA expression levels of TNF- α , IL-6 and CXCL2 at 4 weeks after feeding (Fig. 1A). PG showed no effect on mRNA expression levels of these cytokines in ND-fed mice. In contrast, TNF- α mRNA expression in the adipose tissue was significantly decreased by PG administration in HFD-fed mice. No significant difference was observed in mRNA expression of IL-6 or CXCL2 between the PG-administered group and the control group. We next assessed mRNA expression levels at 8 weeks after feeding (Fig. 1B). In HFD-fed mice, mRNA expression levels of TNF- α , IL-6 and CXCL2 in the PG-administered mice were significantly decreased compared to the control group (Fig. 1B). In ND-fed mice, TNF- α mRNA expression of the PG-administered mice was significantly decreased compared with the control mice.

The proportion of M1 macrophages was decreased by PG administration.

We further examined the population of M1 and M2 macrophages in adipose tissue. After the gating of the F4/80-positive cells from the SVF cells of epididymal adipose tissue, the cells were then analyzed using anti-CD11c and anti-CD206 antibodies as markers of M1 and M2 macrophages, respectively. The population of CD11c⁺F4/80⁺ cells was increased by HFD feeding compared with ND feeding (Fig. 2A). The proportion of CD11c⁺F4/80⁺ cells was significantly decreased by PG administration in HFD-fed mice. In contrast, the proportion of CD206⁺F4/80⁺ cells was not significantly altered by PG administration (Fig. 2B).

M1 macrophages and CLS number were decreased in adipose tissue of PG-administered mice.

Type of ATMs was assessed by immunostaining using anti-F4/80, anti-CD11c and anti-CD206 antibodies. In HFD-fed mice, CD11c⁺F4/80⁺ cells were observed less frequently in the PG-administered mice compared with the control group (Fig. S2A), but frequency of CD206⁺F4/80⁺ cells was not changed (Fig. S2B). As previously reported [15], CD11c⁺F4/80⁺ cells formed CLSs in the epididymal adipose tissue of HFD-fed mice (Fig. S2A), which were rarely observed in that

of ND-fed mice (data not shown). To analyze population of CLSs, we randomly counted CLSs in the immunostained adipose tissue sections. In HFD-fed mice, the CLS number of the PG-administered mice was significantly decreased compared with the control group (Fig. S2C). On the other hand, the CD206⁺F4/80⁺ cell number was not altered by PG administration (Fig. S2D).

PG improved glucose tolerance and serum insulin level.

To assess glucose homeostasis in HFD-fed mice administered with PG, we next performed glucose tolerance test. In HFD-fed mice with PG administration, a significant reduction in blood glucose levels was found at 15 and 30 min after glucose injection (Fig. 3A). Next, we measured fasting insulin levels in serum. As previously described [16], hyperinsulinemia in the HFD-fed mice was shown compared with the ND-fed mice (Fig. 3B). The HFD-fed mice with PG administration exhibited the significantly lower fasting insulin level compared with the control group.

Phosphorylation of Akt stimulated by insulin was enhanced in the liver and gastrocnemius skeletal muscle of HFD-fed mice with PG administration.

As reported previously, phosphorylated Akt is required for activation of insulin signaling [17]. Therefore, we investigated the effect of PG administration on phosphorylation of Akt stimulated with insulin in liver and gastrocnemius skeletal muscle. The band intensity of Akt in HFD-fed mice was comparable to those in ND-fed mice and PG did not alter the band intensity of Akt (Fig. 3A, B). In contrast, enhancement of phosphorylated Akt at Ser473 was observed in the PG-administered group of HFD-fed mice (Fig. 4A, B). After normalization with the band intensity of Akt, the amount of phosphorylated Akt in HFD-fed mice with DW administration was significantly lower than that of ND-fed mice. In addition, the amount of phosphorylated Akt in HFD-fed mice with PG-administered group was significantly higher than that in the control group (Fig. 4C, D).

Discussion

Previous studies have indicated that chronic inflammation is intensively involved in obesity and diabetes [1]. We have reported that PG has an anti-inflammatory effect on mouse models of various inflammatory diseases [11-13]. In addition, we reported that composition of gut microbiota was altered by oral PG administration [14]. In this study, we presented that PG

administration reduced adipocyte size in HFD-induced obesity mice. Gut microbiota is associated with inflammation and changes of adipocyte cell size in adipose tissue [18]. Reduction of adipocyte size may occur by alteration of gut microbiota via PG administration. Additionally, we observed that oral PG administration suppressed mRNA expression of pro-inflammatory cytokines, TNF- α and IL-6, and chemokine such as CXCL2 in obese adipose tissue, suggesting that PG is able to prevent obesity-related inflammation. HFD-induced obesity is associated with increase in M1 macrophages which secrete pro-inflammatory mediators in ATMs [19]. In particular, M1 macrophages, which infiltrate into the adipose tissue of obese rodents and humans, are a major source for proinflammatory cytokines, such as TNF- α and IL-6 [20]. It has been reported that accumulation of M1 macrophages is involved in induction of insulin resistance and that pro-inflammatory cytokines secreted from M1 macrophages directly impair insulin action [21]. Indeed, treatment with omega-3 fatty acids or taurine decreases the ratio of M1 macrophages coincident with increased insulin sensitivity in obese mice [22,23]. Therefore, we analyzed the cells in SVF of epididymal adipose tissues from mice by flow cytometry and found that PG administration reduced the proportion of M1 macrophages in obese adipose tissue. Although significant differences of the body and tissue weights between the control and PG-treated mice

were not found, size of adipocytes was reduced in PG-administered HFD-fed mice. It has been shown that decrease of adipocyte size relates with reduction of inflammatory cytokine production and M1 macrophage proportion [24]. To confirm the effect of PG on proportion of M1 macrophage proportion, we employed immunohistochemical analysis in obese adipose tissue. The number of M1 macrophages and CLSs in obese adipose tissue was decreased by PG administration. These results suggest that PG might decrease or inhibit differentiation or infiltration of M1 macrophages in adipose tissue of HFD-fed mice. For insulin resistance, Akt is a key mediator of glucose metabolism. Akt is clearly involved in glycogen synthesis and suppression of gluconeogenesis in liver and skeletal muscle [25]. We demonstrated that PG administration enhances insulin-stimulated phosphorylation of Akt in the liver and gastrocnemius skeletal muscle. Moreover, PG administration improved glucose tolerance and decreased serum insulin level in HFD-fed mice. These results suggest that PG administration improves the insulin sensitivity and has potency to attenuate type 2 diabetes in obese mice.

In conclusion, we demonstrated that administration with PG reduces the production of pro-inflammatory mediators and the number of M1 macrophages. In addition, PG is able to improve hyperglycemia and insulin sensitivity in obese mice. Our study suggests that PG is a beneficial

material for prevention of obesity-induced disorders.

References

- [1] P. Dandona, A. Aljada, A. Bandyopadhyay, Inflammation: the link between insulin resistance, obesity and diabetes. *Trends Immunol.* 25 (2004) 4-7. PMID: 14698276 doi: 10.1016/j.it.2003.10.013
- [2] S.P. Weisberg, D. McCann, M. Desai, et al., Obesity is associated with macrophage accumulation in adipose tissue. *J Clin Invest.* 112 (2003) 1796-1808. PMID: 14679176 doi: 10.1172/JCI19246
- [3] H. Xu, G.T. Barnes, Q. Yang, et al., Chronic inflammation in fat plays a crucial role in the development of obesity-related insulin resistance. *J Clin Invest.* 112 (2003) 1821-1830. PMID: 14679177 doi: 10.1172/JCI19451
- [4] K.E. Wellen, G.S. Hotamisligil, Obesity-induced inflammatory changes in adipose tissue. *J Clin Invest.* 112 (2003) 1785-1788. PMID: 14679172 doi: 10.1172/JCI20514
- [5] G.S. Hotamisligil, Inflammation and metabolic disorders. *Nature.* 444 (2006) 860-867. PMID: 17167474 doi: 10.1038/nature05485
- [6] F.O. Martinez, S. Gordon, The M1 and M2 paradigm of macrophage activation: time for reassessment. *F1000Prime Rep.* 3 (2014) 6-13. PMID: 24669294 doi: 10.12703/P6-13
- [7] C.N. Lumeng, J.L. Bodzin, A.R. Saltiel, Obesity induces a phenotypic switch in adipose tissue macrophage polarization. *J Clin Invest.* 117 (2007) 175-184. PMID: 17200717 doi: 10.1172/JCI29881
- [8] M. Qatanani, M.A. Lazar, Mechanisms of obesity-associated insulin resistance: many choices on the menu. *Genes Dev.* 21 (2007) 1443-1455.
- [9] E.H. Danen, K.M. Yamada, Fibronectin, integrins, and growth control. *J Cell Physiol.* 189 (2001) 1-13. PMID: 17575046 doi: 10.1101/gad.1550907
- [10] H. Sashinami, K. Takagaki, A. Nakane, Salmon cartilage proteoglycan modulates cytokine responses to *Escherichia coli* in mouse macrophages. *Biochem Biophys Res Commun.* 351 (2006) 1005-1010. PMID: 17094950 doi: 10.1016/j.bbrc.2006.10.146
- [11] T. Mitsui, H. Sashinami, F. Sato, et al., Salmon cartilage proteoglycan suppresses mouse experimental colitis through induction of Foxp3⁺ regulatory T cells. *Biochem Biophys Res Commun.* 402 (2010) 209-215. PMID: 20969831 doi: 10.1016/j.bbrc.2010.09.123
- [12] H. Sashinami, K. Asano, S. Yoshimura, et al., Salmon proteoglycan suppresses progression

- of mouse experimental autoimmune encephalomyelitis via regulation of Th17 and Foxp3⁺ regulatory T cells. *Life Sci.* 91 (2012) 1263-1269. PMID: 23069584 doi: 10.1016/j.lfs.2012.09.022
- [13] S. Yoshimura, K. Asano, A. Nakane, Attenuation of collagen-induced arthritis in mice by salmon proteoglycan. *Biomed Res Int.* 2014 (2014) 406453. PMID: 25032213 doi: 10.1155/2014/406453
- [14] K. Asano, S. Yoshimura, A. Nakane, Alteration of intestinal microbiota in mice orally administered with salmon cartilage proteoglycan, a prophylactic agent. *PLoS ONE.* 8 (2013) e75008. PMID: 24040376 doi:10.1371/journal.pone.0113018
- [15] S. Cinti, G. Mitchell, G. Barbatelli, et al., Adipocyte death defines macrophage localization and function in adipose tissue of obese mice and humans. *J Lipid Res.* 46 (2005) 2347-2355. PMID: 16150820 doi: 10.1194/jlr.M500294-JLR200
- [16] M.S. Winzell, B. Ahrén, The high-fat diet-fed mouse: a model for studying mechanisms and treatment of impaired glucose tolerance and type 2 diabetes. *Diabetes.* 53 (2004) S215-219. PMID: 15561913 doi: 10.2337/diabetes.53.suppl_3.S215
- [17] M. Lu, M. Wan, K.F. Leavens, et al., Insulin regulates liver metabolism in vivo in the absence of hepatic Akt and Foxo1. *Nat Med.* 18 (2012) 388-395. PMID: 22344295 doi: 10.1038/nm.2686
- [18] P. D. Cani, R. Bibiloni, C. Knauf, et al., Changes in gut microbiota control metabolic endotoxemia-induced inflammation in high-fat diet-induced obesity and diabetes in mice. *Diabetes* 57 (2008) 1470-81. PMID: 18305141 doi: 10.2337/db07-1403
- [19] P. Li, M. Lu, M.T.A. Nguyen, et al., Functional heterogeneity of CD11c-positive adipose tissue macrophages in diet-induced obese mice. *J Biol Chem.* 285 (2010) 15333-15345. PMID: 20308074 doi: 10.1074/jbc.M110.100263
- [20] K.E. Wellen, G.S. Hotamisligil, Inflammation, stress, and diabetes. *J Clin Invest.* 115 (2005) 1111-1119. PMID: 15864338 doi: 10.1172/JCI25102
- [21] N. Ouchi, J.L. Parker, J.J. Lugus, et al., Adipokines in inflammation and metabolic disease. *Nat Rev Immunol.* 11 (2011) 85-97. PMID: 21252989 doi: 10.1038/nri2921
- [22] D.Y. Oh, S. Talukdar, E.J. Bae, et al., GPR120 is an omega-3 fatty acid receptor mediating potent anti-inflammatory and insulin-sensitizing effects. *Cell.* 142 (2010) 687-698. PMID: 20813258 doi: 10.1016/j.cell.2010.07.041
- [23] S. Lin, S. Hirai, Y. Yamaguchi, et al. Taurine improves obesity-induced inflammatory responses and modulates the unbalanced phenotype of adipose tissue macrophages. *Mol Nutr*

Food Res. 57 (2013) 2155-2165. PMID: 23939816 doi:10.1002/mnfr.201300150

[24] S. Fujisaka, I. Usui, Y. Kanatani, et al., Telmisartan improves insulin resistance and modulates adipose tissue macrophage polarization in high-fat-fed mice. *Endocrinology*. 152 (2011) 1789-1799. PMID: 21427223 doi: 10.1210/en.2010-1312

[25] P.C. van Weeren, K.M. de Bruyn, A.M. de Vries-Smits, et al., Essential role for protein kinase B (PKB) in insulin-induced glycogen synthase kinase 3 inactivation. Characterization of dominant-negative mutant of PKB. *J Biol Chem*. 273 (1998) 13150-13156. PMID: 9582355 doi: 10.1074/jbc.273.21.13150

Fig. 1. Effect of PG on mRNA expression of proinflammatory cytokines in HFD-fed mice.

Adipose tissue was obtained from ND-fed mice with DW (ND-DW), ND-fed mice with PG (ND-PG), HFD-fed mice with DW (HFD-DW) and HFD-fed mice with PG (HFD-PG) at (A) 4 weeks and (B) 8 weeks after starting of HFD feeding and PG administration. The mRNA expression of TNF- α , IL-6 and CXCL2 was estimated by qRT-PCR (n=7). Asterisks * and ** indicate that *P* value was less than 0.05 and 0.01, respectively.

Fig. 2. Effect of PG on macrophage phenotypes in the adipose tissues of HFD-fed mice.

Cells in SVF were prepared from each group of mice (n=4) at 8 weeks after starting of HFD feeding and PG administration. The cells were stained with FITC-conjugated anti-mouse F4/80 mAb, PE-conjugated anti-mouse CD11c mAb and Alexa647-conjugated anti-mouse CD206 mAb. (A) F4/80⁺CD11c⁺ cells and (B) F4/80⁺CD206⁺ cells were assessed by flow cytometry. An asterisk *

indicates that *P* value was less than 0.05.

Fig. 3. Effect of PG on glucose tolerance and serum insulin levels in HFD-fed mice. (A)

IPGTT was carried out at 14 weeks after starting of HFD feeding and PG administration (n= 6).

(B) Serum insulin levels were determined at 12 weeks after starting of HFD feeding and PG administration (n=6). Asterisks * and ** indicate that *P* value was less than 0.05 and 0.01, respectively.

Fig. 4. Effect of PG on insulin-stimulated Akt phosphorylation in HFD-fed mice.

Phosphorylated Akt in (A) the liver and (B) gastrocnemius skeletal muscle of HFD-fed and ND-fed mice at 12 weeks after starting of HFD feeding and PG administration. Intensity of bands was normalized and expressed as a ratio of pAkt/Akt in (C) the liver and (D) gastrocnemius skeletal muscle. Asterisks * and ** indicate that *P* value was less than 0.05 and 0.01, respectively.

Fig. S1. Effect of PG on HFD-induced obesity. Mice were fed HFD or ND from 4 weeks of age

and they were administered with DW containing 0 or 0.2 mg/ml PG. (A) Body weight and food intake were monitored. (B) Mice were sacrificed and weights of adipose tissue and liver were

measured at 16 weeks after starting of HFD feeding and PG administration. (C) Adipocyte size distribution (%) in ND-fed mice received DW (ND-DW) or PG (ND-PG) and HFD-fed mice received DW (HFD-DW) or PG (HFD-PG) was shown (n=400).

Fig. S2. Immunohistochemical analysis of macrophage phenotypes in the adipose tissue of

HFD-fed mice with or without PG. The adipose tissue of HFD-fed mice was obtained at 8 weeks

after starting of HFD feeding and PG administration. The frozen sections of the tissue were

stained with (A) FITC-conjugated anti-mouse F4/80 mAb and PE-conjugated anti-mouse CD11c

mAb or (B) FITC-conjugated anti-mouse F4/80 mAb and Alexa647-conjugated anti-mouse

CD206 mAb. These cells were counterstained with DAPI (blue). (C) CLSs were randomly

counted from seven sections. (D) F4/80+CD206+ cells were randomly counted from 7 sections.

P value less than 0.01 indicates a significant difference between the PG administered mice and

DW control mice.

Table 1. Primers used to amplify target genes from cDNA

Gene	Primer	Sequence
TNF- α	Forward	5'-GGCAGGTCTACTTTGGAGTCATTGC-3'
	Reverse	5'-ACATTCGAGGCTCCAGTGAATTCGG-3'
IL-6	Forward	5'-TGGAGTCACAGAAGGAGTGGCTAAG-3'
	Reverse	5'-TCTGACCACAGTGAGGAATGTCCAC-3'
CXCL2	Forward	5'-GAACAAAGGCAAGGCTAACTGA-3'
	Reverse	5'-AACATAACAACATCTGGGCAAT-3'
GAPDH	Forward	5'-TGAAGGTCGGTGTGAACGGATTTGG-3'
	Reverse	5'-ACGACATACTCAGCACCAGCATCAC-3'

Fig. 1

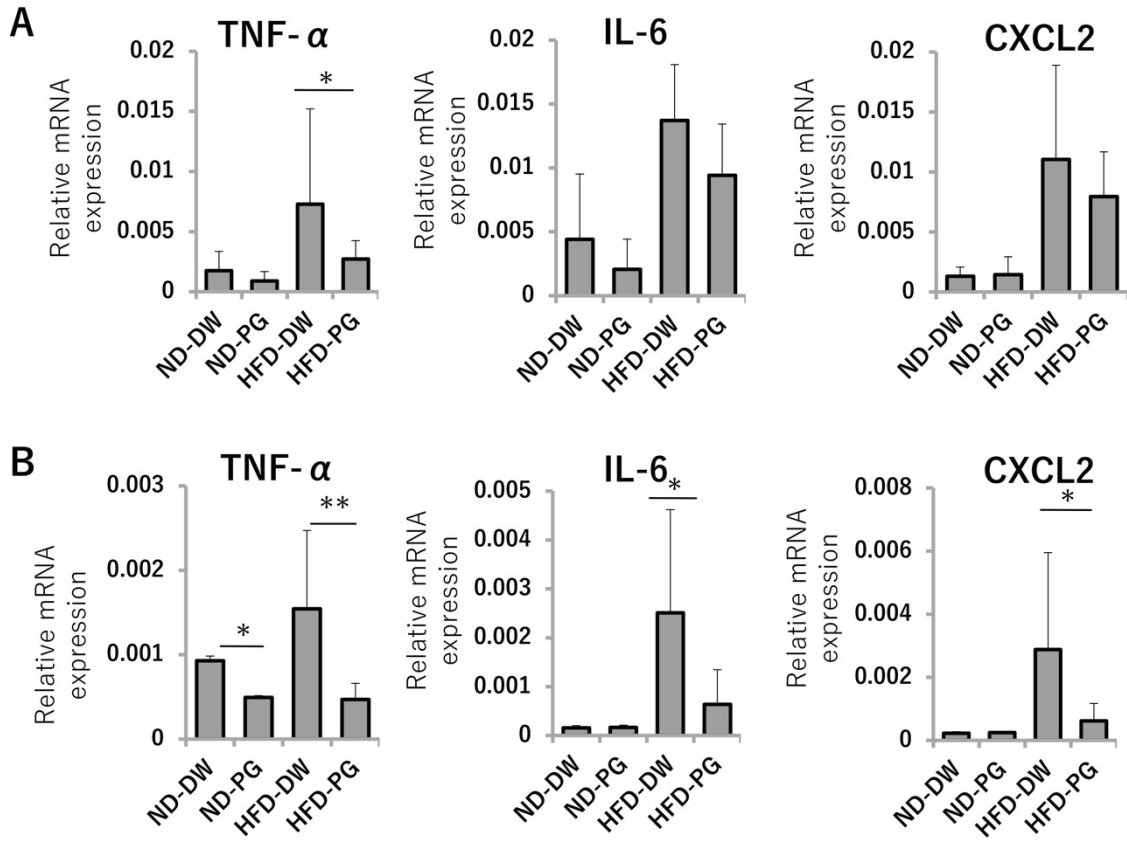


Fig. 2

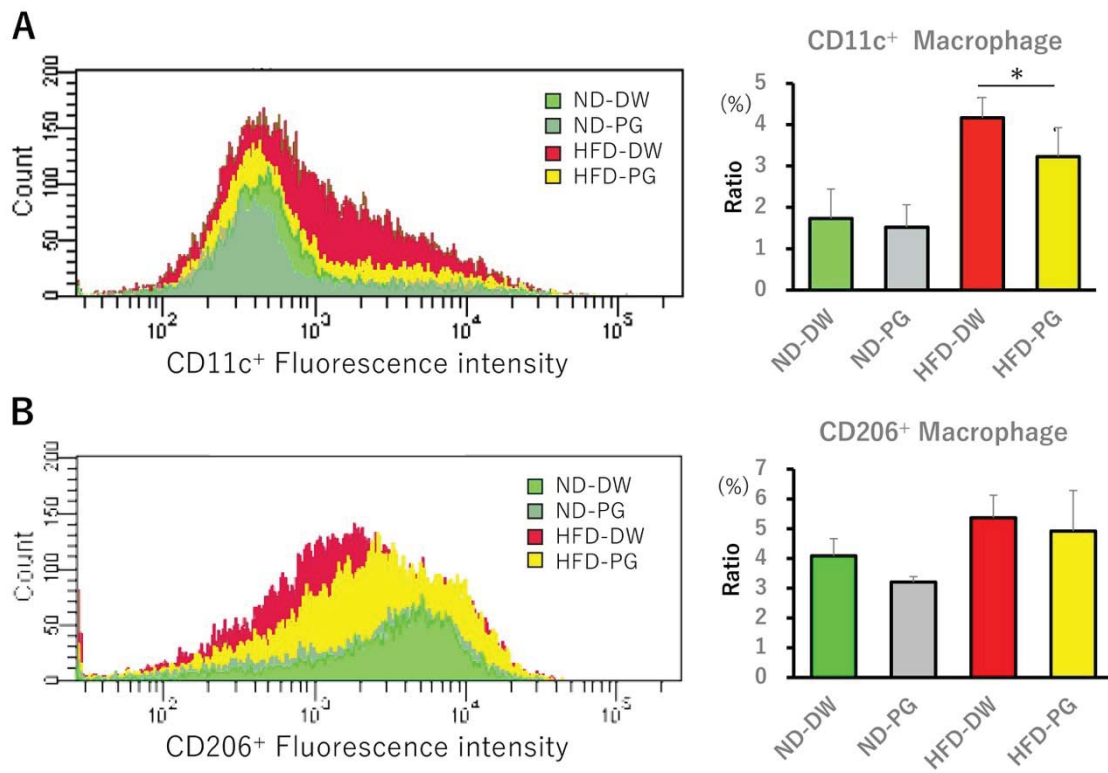
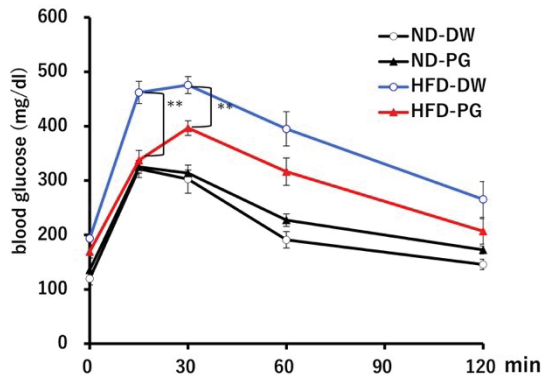


Fig. 3

A



B

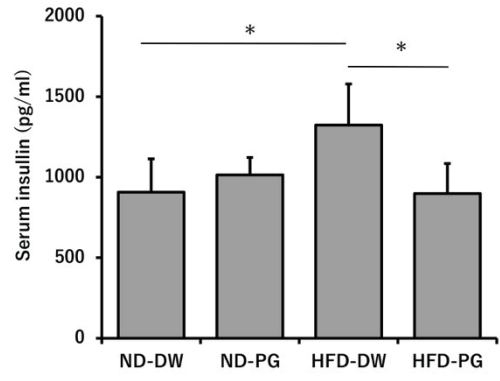


Fig. 4

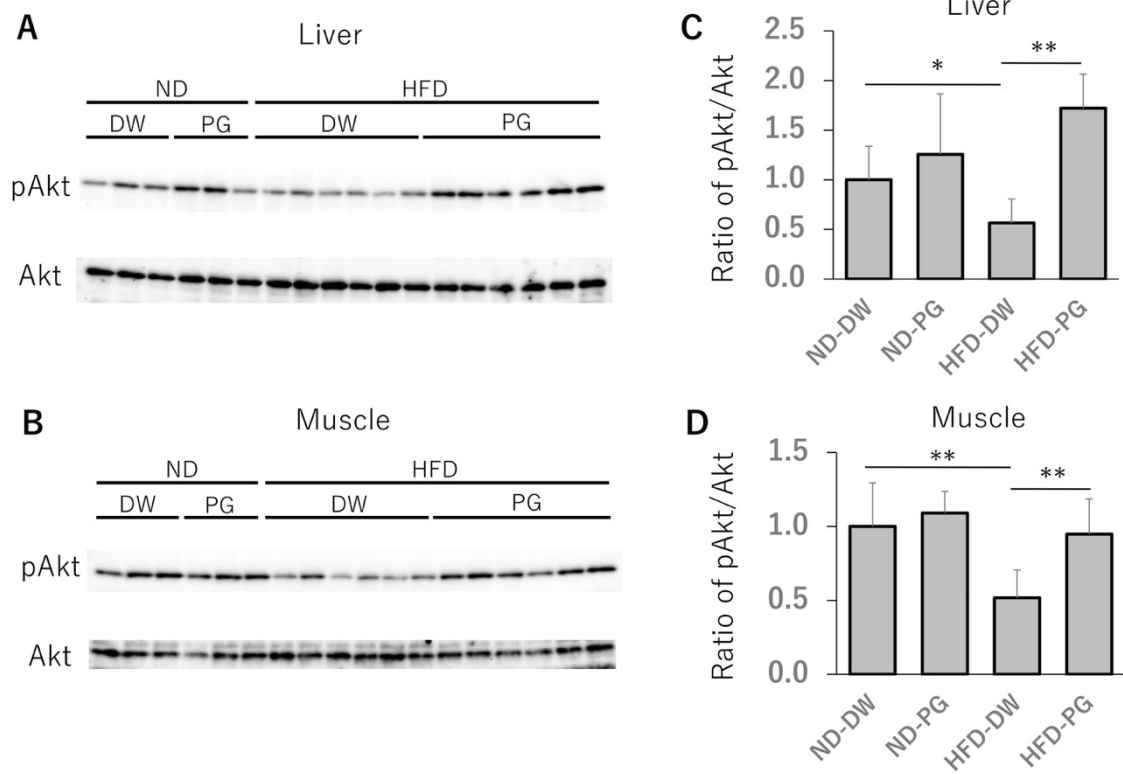


Fig. S1

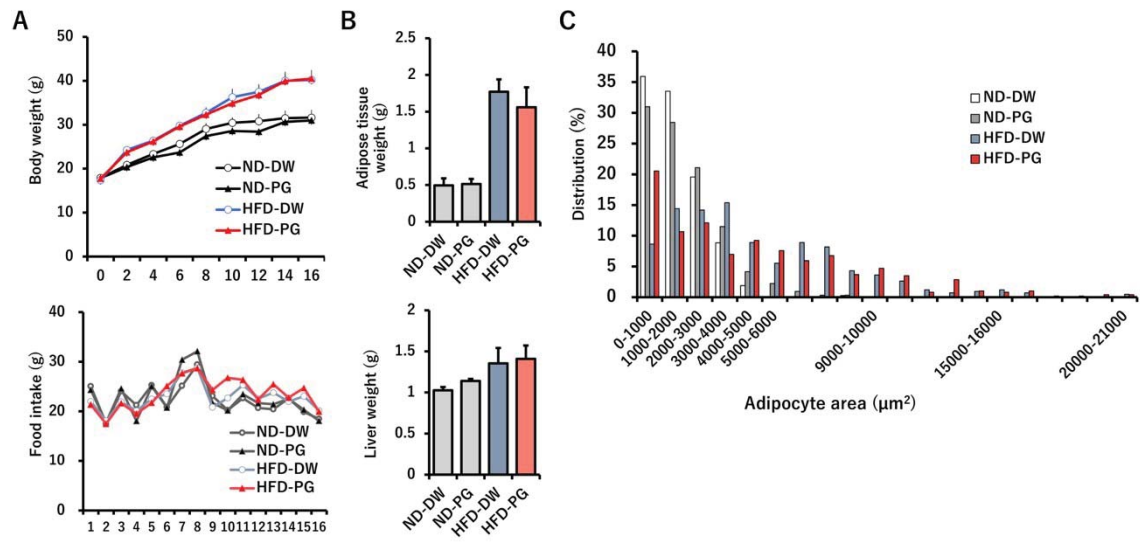


Fig. S2

